10-80-Gb/s highly extinctive electrooptic pulse pattern generation

doi: 10.1109/2944.571763

10–80-Gb/s Highly Extinctive Electrooptic Pulse Pattern Generation

Taiichi Otsuji, *Member, IEEE,* Makoto Yaita, Tadao Nagatsuma, *Member, IEEE,* and Eiichi Sano, *Member, IEEE*

***Abstract*— A pulse-rate-tunable, highly extinctive, ultra-high-speed electrooptic pulse pattern generator has been developed. The optical short pulse generation is based on sinusoidal electrooptic phase modulation and linear chirp compensation using a dispersive medium. Filtering the nonlinear chirp components generated by sinusoidal phase modulation drastically improves the pulse extinction, and makes nearly background-free picosecond pulsation over a wide pulse-rate range even when the group delay dispersion value is fixed.**

I. Introduction

RECENT progress in semiconductor device technology has brought the bandwidth of electronic IC's up into the neighborhood of 100 GHz. In order to test these high-speed chips under actual operating conditions, we have to make large-signal pulse pattern response measurements. Electrooptic sampling (EOS) has a potential detection bandwidth of over 300 GHz, and is recognized as a laboratory-test standard [1]–[3]. Electrooptic pump and probe techniques can provide both subpicosecond temporal resolution and large-signal response measurements [4], but for use in pulse-pattern response measurement, the pulse repetition rate is limited to under 15 Gb/s by the electronic pulse-pattern generator, or PPG. Therefore, practical ultrafast signal sources are urgently required for testing ultrafast photonic and electronic devices [5]–[8]. Pulse-rate tunability and synchronization to electric clocks exciting the device under measurement are essential requirements for characterization use.

Sinusoidal electrooptic phase modulation of around π radians and linear chirp compensation makes pulse compression of 0.1 (*relative to the modulation period*) or less from a CW laser light possible [9]. By quadruplexing the bit rates, we have achieved 10–72-Gb/s tunability using an 18-GHz bandwidth $LiNbO_3$ phase modulator and a dispersion shifted fiber [6]. The problem is the nonuniform, insufficient extinction ratio varying from 13.5 to 20 dB with the bit rate [10], which seriously degrades the pulse eye-opening.

This paper addresses a technique to improve the extinction ratio (to beyond 20 dB) for the electrooptic pulse pattern generator with a wide pulse-rate tunable range. Section II overviews the system configuration. An optical bandpass filter is introduced to improve the pulse extinction. In Section III, the relation between pulse parameters including the filter bandwidth and the pulse waveforms are theoretically investigated. In Section IV, the effect of the filter on the extinction is experimentally verified at pulse rates up to 80 Gb/s. The measured results are also discussed.

Manuscript received September 13, 1996; revised January 8, 1997.

The authors are with NTT System Electronics Laboratories, 3-1 Morinosato Wakamiya, Atsugi, Kanagawa 243-01, Japan.

Publisher Item Identifier S 1077-260X(96)09677-3.

II. System Configuration

A block diagram of the developed generator is shown in Fig. 1. The PPG consists of three blocks, namely, the optical pulsation block, the optical data formatting block, and the electrical control block. In the optical pulsation block, picosecond optical pulses are basically generated by electrooptic phase modulation (PM) and dispersion compensation using a highly-dispersion shifted fiber (HDSF). The amplitude modulation (AM) prior to the PM is an additional preformation to improve the extinction. The bandwidth-tunable optical bandpass filter is newly added in the original generator [10]. This is the key to highly extinctive pulsation over a wide range of pulse rates.

After continuous return-to-zero, or RZ pulsation, a specific pulse pattern train is obtained by modulating the amplitude in accordance with the electrical pattern data. The bit rate of the pulse train can be duplexed or quadruplexed by the optical time-division multiplexer (TDM) block.

The features of this electrooptic PPG are 1) pulse-rate tunability; 2) synchronization with RF signals; 3) very low timing jitter; 4) optical power-independent pulsation; 5) electrical pulsation control; 6) peak power gain; and 7) high extinction ratio. The first three are fundamental requirements of testing tools. The next three contribute to practical instrumentation. The last one is the result of this study.

III. Theory

A. Principle of Highly Extinctive Electrooptic Short Pulse Generation

A CW beam from a laser diode is electrooptically phase modulated by a sinusoidal signal. This makes harmonic sidebands around the optical carrier frequency, and repetitive positive and negative frequency chirping in every modulation frequency period as shown in Fig. 2(a). Either the positive or the negative chirping can be compensated for by passing the beam through a dispersive medium. This causes the bunching of the optical frequency components.

One problem with this pulsation is the remaining dc floor level. This is caused by the positive or negative chirp components that do not contribute to the bunching. Furthermore, since the frequency chirp is not linear, linear chirp compensation yields undesirable wings around the main pulses. These two things considerably degrade the pulse extinction ratio.

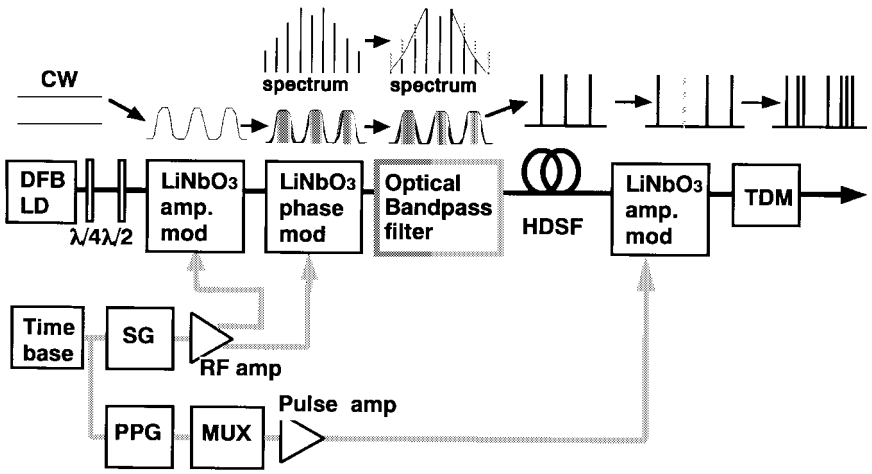

Fig. 1. Optoelectronic pulse-pattern generator. HDSF: highly dispersion shifted fiber; TDM: time division multiplexer; SG: synthesized signal generator; and PPG: electronic pulse pattern generator.

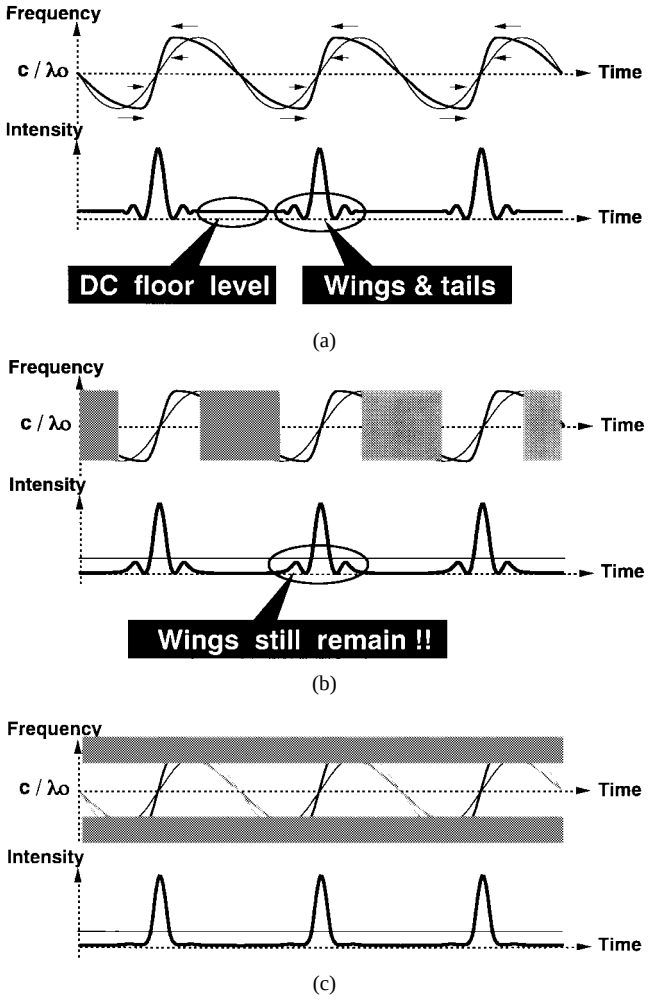

Fig. 2. Principle of electrooptic short pulse generation: (a) PM only, (b) PM & AM, and (c) PM & AM & optical bandpass filtering.

One way to suppress the dc floor level is sinusoidal amplitude modulation [9], which removes the inverse chirp components in every phase modulation period [see Fig. 2(b)]. We also employed it. However, note that the wings still remain.

The frequency chirp becomes more nonlinear as the optical frequency moves away from the center frequency. This indicates, as shown in Fig. 2(c), that passing the optical spectrum through a bandpass filter can suppress the nonlinear chirp components. Either a Fabry–Perot etalon or a Mach–Zehnder interferometer can be used for this. Assuming a phase modulation frequency of 10–20 GHz and a modulation index of around π radians, spectral widths range from 50 to 150 GHz. Therefore, the filter has to be tunable over a bandwidth from tens to hundreds of gigahertz.

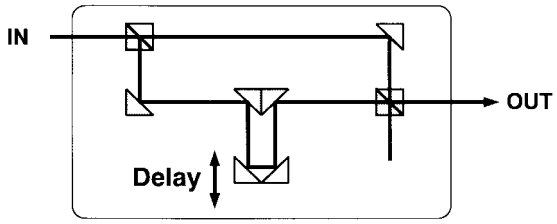

Fig. 3. Bandwidth-tunable Mach–Zehnder interferometric optical bandpass filter.

B. Analysis

The filter we tried is a bandwidth-tunable Mach–Zehnder interferometric filter (MZI) as shown in Fig. 3. The MZI consists of a pair of beam splitters and a variable delay line. According to the desired bandwidth (20–150 GHz for 10–20-GHz repetition), the delay value is controlled in an mm range. The center frequency can be tuned by finely controlling the delay value with submicron resolution. When the filter center frequency is tuned to the optical carrier frequency, its transfer T_{MZI} is expressed as

$$T_{\mathrm{MZI}} = 1 - S \sin^2\left[\frac{\pi n f_m}{(2\mathrm{BW}_{\mathrm{MZI}})}\right] \tag{1}$$

where S is the MZI filter modulation depth, n the harmonic number of the spectrum, f_m the phase modulation frequency, and $\mathrm{BW}_{\mathrm{MZI}}$ the filter bandwidth.

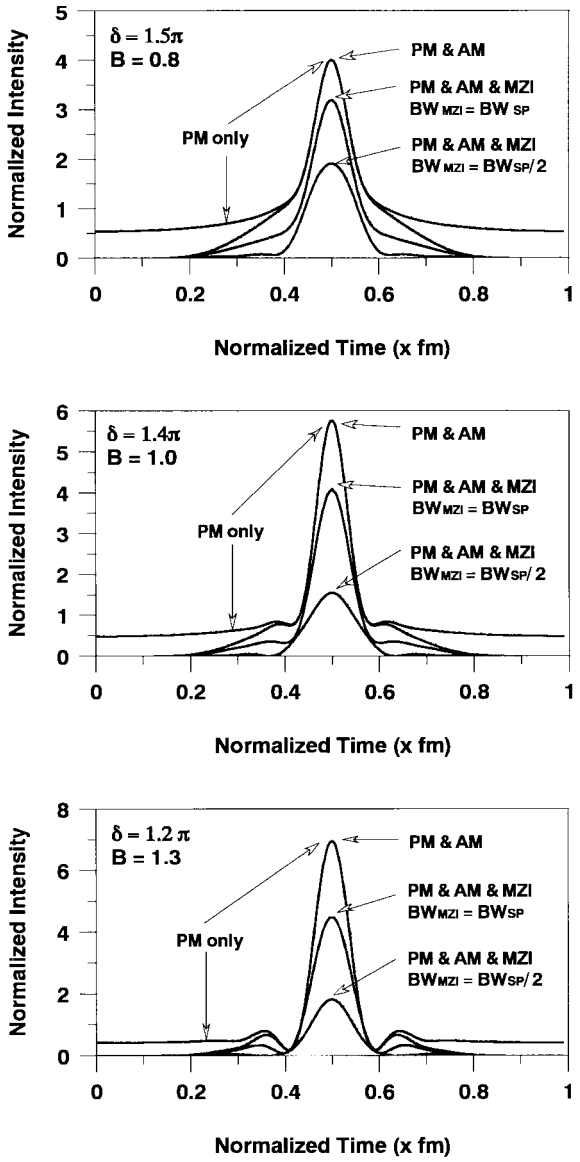

Fig. 4. Calculated pulse waveforms for different δ and B values. $\mathrm{BW_{MZI}}$: the filter bandwidth, $\mathrm{BW_{SP}}$: the optical spectral width. The vertical axis is normalized to the average power of the incident CW light.

The envelope of the generated optical pulse intensity, $|E_0(t)|^2_{\text{envelope}}$, is expressed as follows:

$$
\begin{aligned}
&|E_0(t)|2_{\text{envelope}} \\
&\quad \propto \left\{1 - S\sin^2\left[\frac{\pi n f_m}{(2\mathrm{BW_{MZI}})}\right]\right\} \\
&\qquad \cdot \left|\sin\left\{\frac{\pi}{4}\left[1 - \Gamma_m \sin(2\pi f_m t)\right]\right\} \times \sum_{n=-\infty}^{\infty} J_n(\delta)\right. \\
&\qquad \left. \cdot \exp\left\{-j2\pi f_m\left[t - \tau(\omega_o)\right] - \frac{nB\delta}{2}\right\}\right|^2 \\
&B = -\left(\frac{\partial\tau}{\partial t}\right)_{\max} \times (\mathrm{GDD}) \\
&\quad = \pm 2\pi f_m^2 \delta\left(\frac{\lambda^2}{c}\right)\left(\frac{\partial\tau}{\partial\lambda}\right) \qquad (2)
\end{aligned}
$$

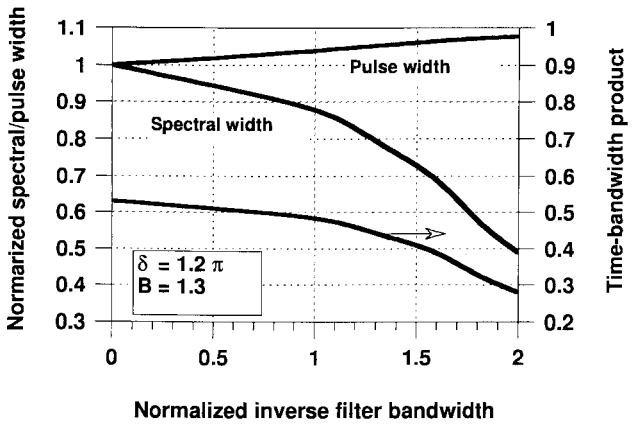

Fig. 5. Calculated pulse parameters versus inverse filter bandwidth (normalized to the optical spectral width) for $\delta = 1.2\pi$ and $B = 1.3$.

where Γ_m is the sinusoidal amplitude modulation depth, J_n the nth Bessel function, f_m the phase modulation frequency, δ the phase modulation index, $\tau(\omega) = \partial\theta/\partial\omega$ the group delay, λ the wavelength, c the speed of light, and B the bunching parameter [the product of the frequency chirping rate and the group delay dispersion (GDD)]. An optimum bunching condition is given by $B = 1$ where the frequency chirping caused by PM is optimally compensated for. A B value of less/greater than 1 means under/over chirp compensation [9].

From (2), we see that the pulse waveform can be expressed as a function of δ and B when it is normalized to f_m. Thus, the effect of filtration on pulse waveform was investigated with δ and B as parameters. Typical results of calculated pulse waveforms for several δ and B conditions are shown in Fig. 4(a)–(c). Simple PM shows both a dc floor level and wings. Sinusoidal AM effectively suppresses residual DC floor levels [9], [10] while maintaining the pulse height, but the wings still remain. When the bandwidth of the MZI is narrowed to half of the optical spectral width ($\sim 2\delta f_m$), the wings almost disappeared, and the ratio of main pulse height to wing height drastically improves over a wide B range from 0.8 to 1.3. The pulse peak power still exceeds the average incident CW power.

It is also noted that, in comparison with Fig. 4(b) and (c), the pulse compression ratio after filtration for $\delta = 1.4\pi$ and the optimum bunching ($B = 1$) is lower than that for a less δ of 1.2π and overcompensation ($B = 1.3$). This indicates that the optimum pulsation condition yielding shorter pulsewidth and smaller wings, with and without optical filtration is different in each case.

Fig. 5 shows the pulse parameters versus the inverse filter bandwidth (normalized to the incident spectral width) for $\delta = 1.2\pi$ and $B = 1.3$. Note that the time bandwidth product (TBP) decreased from 0.53 (without filtration) to less than 0.30 as the filter bandwidth narrowed to half the spectral width. Thus, a background-free soliton-like pulse (TBP = 0.32) can be generated by bandpass filtration. This is the result of effective spectral narrowing while mostly maintaining the pulsewidth.

When the filter bandwidth is not much narrower than half the spectral width, the pulsewidth τ can roughly be estimated by the following semi-empirical formula derived for pure-PM

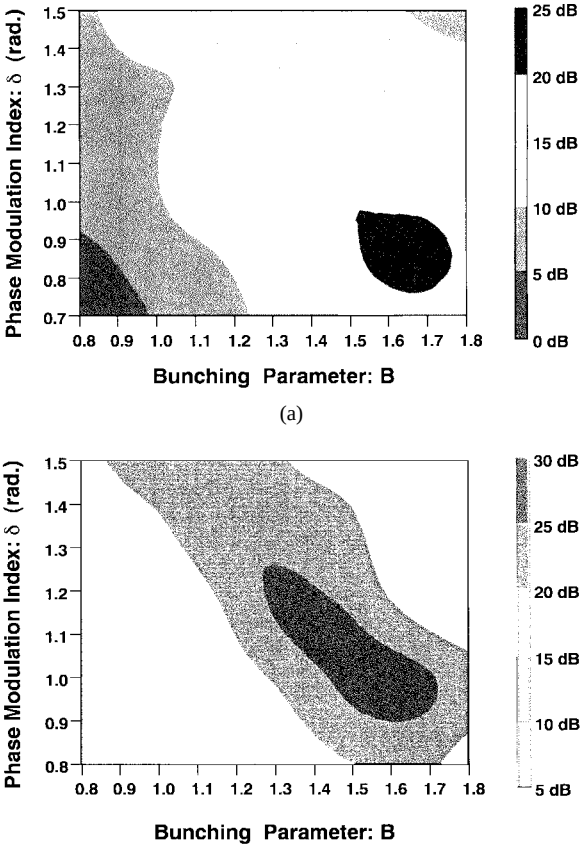

Fig. 6. Extinction ratio versus δ and B for quadruplexed repetitive "$10110100\cdots$" pattern. (a) PM & AM and (b) PM & AM & MZI.

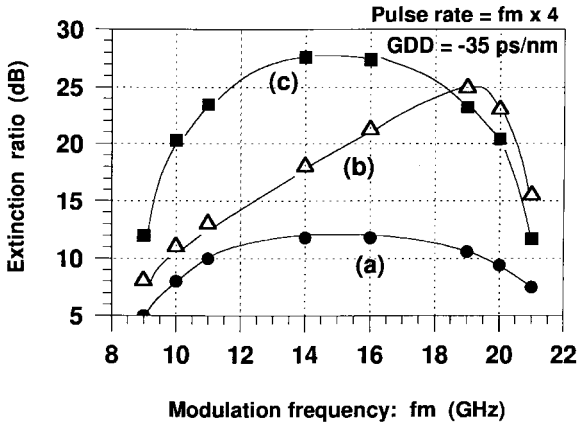

Fig. 7. Extinction ratio versus fundamental phase modulation frequency for quadruplexed repetitive "$10\,110\,100\cdots$" pattern. (a) PM only, (b) PM & AM, and (c) PM & AM & MZI.

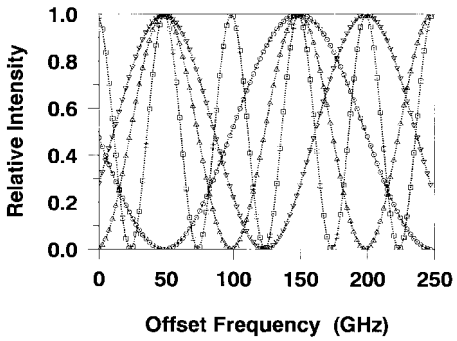

Fig. 8. Transfer of a dedicated MZI filter at pass-bandwidths of 25, 50, and 100 GHz.

pulsation [6]:

$$\tau = \frac{B^{0.27} + 0.03B^{-2.9} - 0.59}{2\delta\theta^{\exp(-0.34B^{-2.24})} f_m}. \tag{3}$$

Assuming today's $LiNbO_3$ modulators with $V\pi$ of $\sim$5 V and RF power amplifiers with a 1-W saturation, obtainable δ is limited to less than 2π. Even if the GDD value is fixed under such a weak δ condition, we expect that a wingless pulse compression to 0.1 or less can be performed in a wide f_m range from a lower limit frequency f_0 to twice the f_0. This is very important for practical instrumentation where the pulse rate is to be quadruplexed, since it is hard to control the GDD value electrically.

The pulse extinction ratio versus δ and B in the case of a quadruplexed repetitive "$10110100\cdots$" pattern was calculated. The filter bandwidth was optimized to obtain the best extinction for each δ and B condition. This is shown in Fig. 6. When the pulsation occurs without MZI, a good extinction ratio of $>$20 dB is obtained only in a very restricted region of $\delta \approx 0.8\pi$ and $B \approx 1.6$. Introduction of the MZI to PM and AM drastically enlarges the δ and B range that achieves $>$20-dB extinction.

Fig. 7 shows the calculated extinction ratio versus f_m in the case of a quadruplexed repetitive "$10110100\cdots$" pattern. The GDD was set to be an optimum value of -35 ps/nm so as to cover the f_m range from 10 to 20 GHz. δ and B values as well as the filter bandwidth were optimized to obtain the best extinction for each f_m. Pure sinusoidal PM gives nearly 10-dB extinction. The addition of sinusoidal AM partially improves the extinction, but it is strongly f_m-dependent. In contrast, AM & PM & MZI can maintain over 20-dB extinction in the f_m range from 10 to 20 GHz. This indicates that the good extinction is obtained at pulse rates from 10 to 80 Gb/s. From this result, the optimum GDD value for obtaining a tunable range from f_m to $2f_m$ is given in a general form as

$$\text{GDD} = \frac{\pm 28.0\, c}{f_m^2 \lambda^2} \text{ (ps/nm)}. \tag{4}$$

IV. Experiments

A. Measurement Setup

In order to verify the analytical results, we conducted some experiments on pulse pattern generation and measurement. The optoelectronic components in the electrooptic PPG are the same as those in [10] except for the newly added MZI filter.

The measured transfer characteristics of the dedicated MZI filter are shown in Fig. 8 as a function of the delay value. A good extinction ratio of over 25 dB is obtained over the pass-bandwidth from tens of gigahertz to hundreds of terahertz. Its transfer characteristics also coincides well with the theoretical ones.

We prepared two measurement setups: one for low bit-rate measurements at around 40 Gb/s, and the other for higher bit-

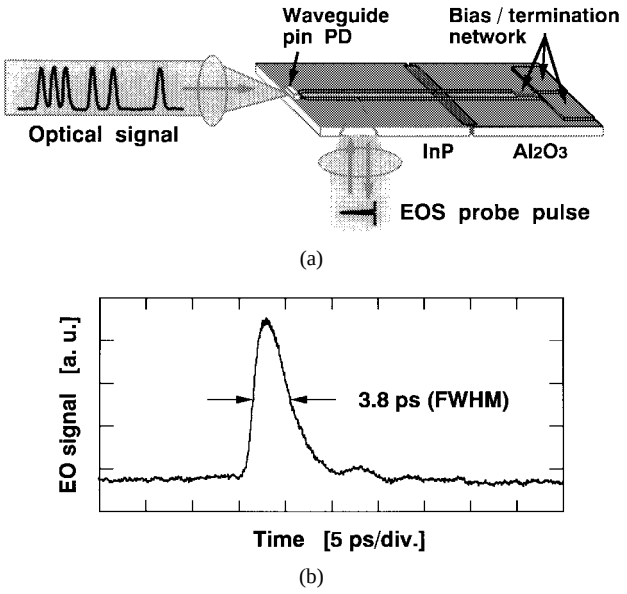

Fig. 9. 100-GHz bandwidth optical signal sampler: (a) block diagram and (b) impulse response measured with a 350-fs-wide soliton pulse.

rate measurements. The former included a 40-GHz bandwidth p-i-n photodiode (ν-104) and a 50-GHz bandwidth electronic digitizing oscilloscope (HP-54 124T). For the measurement of an ultrafast optical pulse pattern waveform, a dedicated 100-GHz-bandwidth optical signal sampler [11], [12] was used. The block diagram of the optical sampler is shown in Fig. 9(a). It consists of a wide-band waveguide p-i-n photodiode, an electrooptic sampling head, and a bias/termination network. The EOS head is made of a 50-Ω coplanar waveguide on an InP substrate. The InP substrate acts as an ultrafast electrooptic transducer.

First, we measured the impulse response of the sampler itself [see Fig. 9(b)] using a 350-fs-wide soliton pulse [12]. Then, we measured the target pulse pattern waveforms. Finally, we deconvolved the sampler response from the measured waveforms. The sampler itself had a 3-dB bandwidth of 100 GHz.

B. Results and Discussion

By setting the optimum GDD value to -35 ps/nm, we tried to generate the quadruplexed "$10110100\cdots$" pulse pattern in the f_m range from 10 to 20 GHz. As seen in Fig. 6, the extinction ratio is critical at the lower and upper limits of f_m. Typical results for these critical bit rates of 40 (10×4) and 80 (20×4) Gb/s are shown in Figs. 10 and 11. Fig. 10 shows the waveforms at 40 Gb/s ($f_m = 10$ GHz) measured by the electronic digitizing oscilloscope. The δ and B values were set at 1.5π and 0.83. The large δ but insufficient GDD value makes large dull wings in spite of a rather short pulsewidth, which results in a considerably worse extinction of about 5 dB for pulsation without MZI [see Fig. 10(a)]. When the MZI bandwidth narrows to 55 GHz, the bottom level between the successive "1" pattern almost reaches the original zero level. The large overshoot at falling transition just before the successive "0" pattern is due to the undesireble peaking characteristics of the p-i-n photodiode used in this

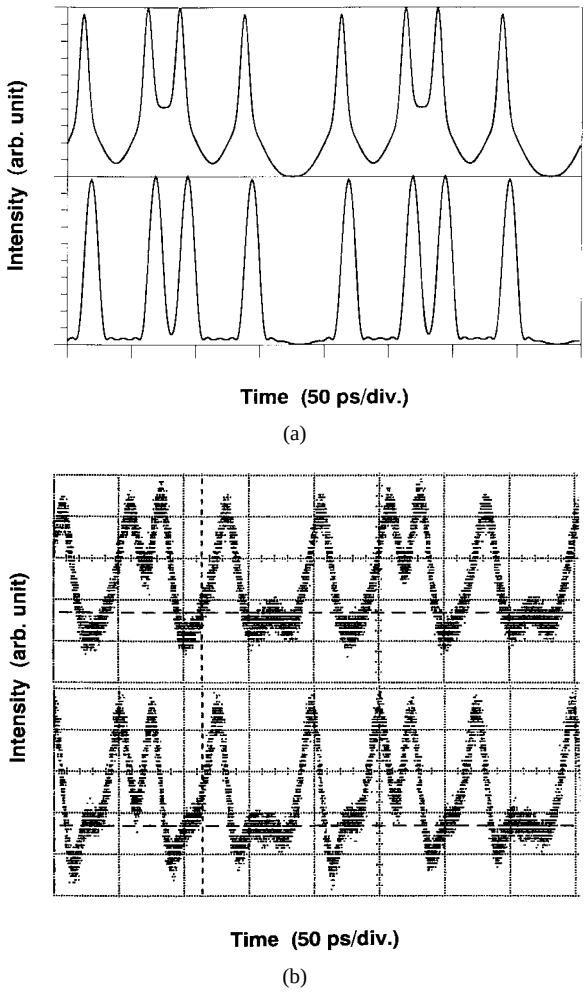

Fig. 10. Pulse pattern waveforms for a 40-Gb/s RZ "$10110100\cdots$" repetitive pattern. $f_m = 10$ GHz, $\delta = 1.5\pi$, GDD $= -35$ ps/nm. Upper trace: PM&AM; lower trace: PM&AM&MZI ($\mathrm{BW_{MZI}} = 55$ GHz). (a) Calculated and (b) measured.

measurement. The extinction ratio of the measured signal is estimated to be over 20 dB.

Fig. 11 shows the waveform at 80 Gb/s ($f_m = 20$ GHz). The δ and B values were set at 0.8π and 1.77. As seen in Fig. 6, at this upper f_m-limit condition, MZI can no longer work effectively, and so it was eliminated. In contrast with Fig. 10, the small δ and large B value creates a relatively large pulsewidth with small satellite pulses that contribute to a good extinction of over 20 dB. For both cases in Figs. 10 and 11, measured waveforms almost coincide with the calculated ones. The residual pulse-height variation is attributed to the unequal dividing ratio of the TDM used in this experiment. Small disagreements in the pulse-to-pulse distances are due to misalignment in the TDM. Throughout this experiment, good extinction ratios over 20 dB were confirmed over the pulse-rate range of 10–80 Gb/s.

In order to demonstrate the effect of MZI on extinction at a relatively high bit rate, another experiment was conducted. A 72-Gb/s "$10110100\cdots$" pattern was generated for AM&PM and AM&PM&MZI. The pulsation conditions were $f_m = 18$ GHz, $\delta = 1.2\ \pi$, and GDD $= -14$ ps/nm. The GDD was intentionally set to a nonoptimum value to provide insufficient

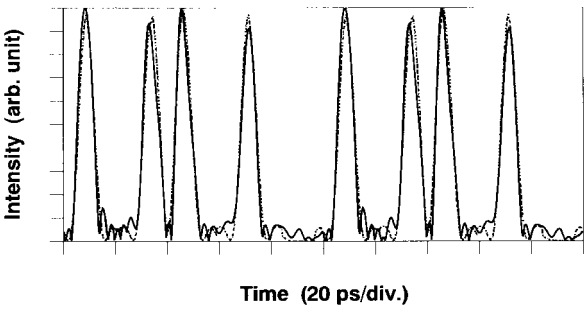

Fig. 11. Measured pulse pattern waveforms for a 80-Gb/s RZ "10110100$\cdots$" repetitive pattern for PM and AM (MZI filter is not used). $f_m = 20$ GHz, $\delta = 0.8\pi$, GDD $= -35$ ps/nm. Solid lines: Measured. Dashed lines: Calculated.

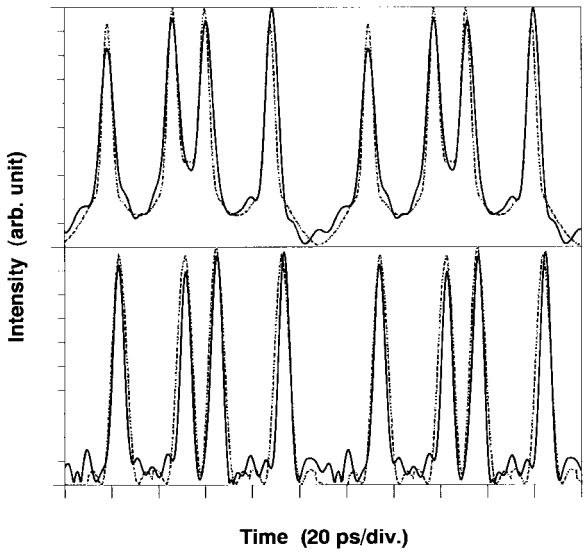

Fig. 12. Measured pulse pattern waveforms for a 72-Gb/s RZ "10110100$\cdots$" repetitive pattern. $f_m = 18$ GHz, $\delta = 1.2\pi$, GDD $= -14$ ps/nm. Upper trace: PM&AM; lower trace: PM&AM&MZI ($\mathrm{BW_{MZI}} = 68$ GHz). Solid lines: Measured. Dashed lines: Calculated.

chirp compensation. The optical pulse pattern waveforms measured by the optical signal sampler are shown in Fig. 12 (deconvolved results). The extinction ratio for the waveform without filtering was 10.2 dB. The residual wings degraded both the low-level extinction and the uniformity of the pulse peak height. In contrast, by reducing the MZI bandwidth to 68 GHz (= half the spectral width), the residual wings were further suppressed, resulting in a better extinction ratio of 20.5 dB.

For both cases in Figs. 11 and 12, the residual floor noise is slightly larger than that in the calculated results. The electrical signal distortions due to the harmonics and multiple-reflection of the microwave amplifier for driving the modulators are thought to be the main cause. Analytical error in deconvolving the sampler response should also be considered.

Currently, the maximum pulse rate is limited by the bandwidth of the $LiNbO_3$ modulators ($\sim$18 GHz at -3 dB) used in this experiment. At the research level, the bandwidth and $V\pi$ of the modulator are now approaching 100 GHz and 3.0 V [13]. The next bottleneck is the bandwidth of the solid-state microwave power amplifier. Recently, a V-band, 0.5-W MMIC power amplifier has been developed [14]. Assuming these technological advancements, generation of 200-Gb/s pulse pattern (4×50 Gb/s) will be practicable in the very near future.

V. Conclusion

We demonstrated a widely pulse-rate-tunable, highly-extinctive, practical ultra-high-speed electrooptic pulse pattern generator. A bandwidth-tunable, Mach–Zehnder interferometric optical bandpass filter was introduced to the original generator based on electrooptic phase modulation and frequency-chirp compensation. Filtering the nonlinear chirp components generated by sinusoidal electrooptic phase modulation makes a highly extinctive, nearly background-free picosecond pulsation possible. Analytical results suggested that a good extinction of $>$20 dB (electrical) could be obtained over a wide pulse-rate range from a lower limit rate f_0 to 8 f_0 by time-division quadruplexing the pulse rate. Using a set of 18-GHz bandwidth $LiNbO_3$ modulators and a single dispersion shifted fiber having a group delay dispersion of -35 ps/nm, a repetitive pulse pattern was generated at pulse rates from 10 to 80 Gb/s. A good extinction ratio of $>$20 dB was experimentally verified over that pulse-rate range. This proposed technique will become indispensable for practical pulse pattern generators used in testing ultrafast electronic/photonic devices.

Acknowledgment

The authors would like to thank S. Horiguchi, O. Karatsu, Y. Akazawa, and K. Matsuhiro for their direction and encouragement. The authors are also much indebted to M. Yoneyama for his valuable discussions.

References

[1] H. Cheng and J. F. Whitaker, "300-GHz-bandwidth network analysis using time-domain electrooptic sampling," in *Tech. Dig. IEEE MTT-S Int. Microwave Symp.*, 1993, pp. 1355–1358.
[2] T. Nagatsuma, "Measurement of high-speed devices and integrated circuits using electrooptic sampling technique," *IEICE Trans. Electron.*, vol. E76-C, no. 1, pp. 55–63, 1993.
[3] M. Y. Frankel, "Optoelectronic techniques for ultrafast device network analysis to 700 GHz," *Opt. Quantum Electron.*, vol. 28, no. 7, pp. 783–800, 1996.
[4] M. J. W. Rodwell, M. Riaziat, K. J. Weingarten, B. A. Auld, and D. M. Bloom, "Internal microwave propagation and distortion characteristics of traveling-wave amplifiers studied by electrooptic sampling," *IEEE Trans. Microwave Theory Tech.*, vol. 34, no. 12, pp. 1356–1362, 1986.
[5] W. H. Knox, "What will be the impact of ultrafast science and technology in the real world?," in *Proc. 1994 IEEE LEOS Annu. Meet.*, 1994, vol. 1, pp. 303–304.
[6] T. Otsuji, K. Kato, T. Nagatsuma, and M. Yoneyama, "10 to 72-Gb/s, optoelectronic RZ pulse-pattern generation and its application to on-wafer large-signal characterization for ultra-high-speed electronic devices," in *Proc. 1994 IEEE LEOS Annu. Meet.*, vol. 2, pp. 203–204, 1994.
[7] J. J. Veselka and S. K. Korotky, "Optical soliton generation based on a single Mach–Zehnder modulator," in *Tech. Dig. Integrated Photon. Res.*, 1994, pp. 190–192.
[8] S. V. Chernikov, J. R. Taylor, I. Samartsev, and V. P. Gapontsev, "Compact all-diode-pumped fiber-optical pulse sources at 35–80 Gb/s," in *Proc. 1995 OFC*, 1995, pp. 294–295.
[9] T. Kobayashi, H. Yao, K. Amano, Y. Fukushima, A. Morimoto, and T. Sueta, "Optical pulse compression using high-frequency electrooptic phase modulation," *IEEE J. Quantum Electron.*, vol. 24, no. 2, pp. 382–387, 1988.

[10] T. Otsuji, T. Nagatsuma, K. Kato, and M. Yoneyama, "Widely tunable electrooptic pulse-pattern generation and its application to on-wafer large-signal characterization of ultra high-speed electronic devices," *Opt. Quantum Electron.*, vol. 28, no. 7, pp. 991–1005, 1996.
[11] M. Yaita, T. Nagatsuma, K. Kato, T. Otsuji, and Y. Muramoto, "Ultrafast optical pulse-pattern signal measurement using optoelectronic techniques," in *Tech. Dig. CLEO/Pacific Rim '95*, 1995, p. 217.
[12] M. Yaita, T. Nagatsuma, K. Suzuki, K. Iwatsuki, K. Kato, and Y. Muramoto, "Ultrafast optical pulse-pattern signal measurement using optoelectronic techniques," *Electron. Lett.* vol. 31, no. 17, pp. 1501–1502, 1995.
[13] K. Noguchi, O. Mitomi, and H. Miyazawa, "Low-voltage and broadband Ti:$LiNbO_3$ modulators operating in the millimeter wavelength region," in *Tech. Dig. OFC '96*, 1996, pp. 205–206.
[14] O. Tang, K. Duh, S. Liu, P. Smith, W. Kopp, T. Rogers, and D. Ptitchard, "A 560-mW, 21% power-added efficiency V-band MMIC power amplifier," in *Tech. Dig. GaAs IC Symp.*, 1996, pp. 115–118.

Taiichi Otsuji (M'91) was born in Fukuoka, Japan, on September 5, 1959. He received the B.S. and M.S. degrees in electronic engineering from Kyushu Institute of Technology, Fukuoka, Japan, in 1982 and 1984, respectively, and the Ph.D. degree in electronic engineering from Tokyo Institute of Technology, Tokyo, Japan, in 1994.

In 1984, he joined the Electrical Communication Laboratories, NTT, Japan, where he engaged in the research and development of high-accuracy timing generation and calibration LSI's for LSI test systems. His current research interest includes ultra-broard-band electronic IC design and ultrafast optoelectronic measurement technologies.

Dr. Otsuji is a member of IEEE Lasers and Electro-Optics Society, Optical Society, and the Institute of Electronics, Information, and Communication Engineers of Japan.

Makoto Yaita was born in Saitama, Japan, in 1966. He received the B.S. and M.S. degrees in chemistry from Waseda University, Tokyo, Japan, in 1988 and 1990, respectively.

In 1990, he joined LSI Laboratories, Nippon Telegraph and Telephone (NTT) Corporation, Kanagawa, Japan. He has been engaged in the research and development of measurement and test technology of high-speed semiconductor devices and LSI's.

Mr. Yaita is a member of the Institute of Electronics, Information, and Communication Engineers of Japan, and the Japan Society of Applied Physics.

Tadao Nagatsuma (M'93) received the B.S., M.S., and Ph.D. degrees in electronic engineering from Kyushu University, Fukuoka, Japan, in 1981, 1983, and 1986, respectively.

He joined the Nippon Telegraph and Telephone Corporation (NTT), Atsugi Electrical Communications Laboratories, Kanagawa, Japan. His current research involves design, characterization, and testing of high-speed semiconductor devices and circuits, and optical probing of ultrafast electronics.

Dr. Nagatsuma is a member of the Japan Society of Applied Physics, the Institute of Electronics, Information, and Communication Engineers (IEICE) of Japan, and the Optical Society of America. He was the recipient of the 1989 Young Engineers Award from IEICE, and the 1992 Andrew R. Chi Best Paper Award.

Eiichi Sano (M'84) was born in Shizuoka, Japan, on December 4, 1952. He received B.S. and M.S. degrees from the University of Tokyo, Tokyo, Japan, in 1975 and 1977, respectively.

In 1977, he joined the Electrical Communication Laboratories, NTT, Tokyo, Japan. He has been engaged in the research on MOS device physics, performance limits of mixed analog/digital MOS ULSI's, ultrafast MSM photodetectors and electro-optic sampling for measuring high-speed devices. His current research interests include high-speed electronic and optoelectronic devices for optical communication.

Mr. Sano is a member of the Institute of Electronics, Information and Communication Engineers of Japan.